A REVERSIBLE DATA HIDING METHOD BY HISTOGRAM SHIFTING IN HIGH QUALITY MEDICAL IMAGES

LI-CHIN HUANG [3], LIN-YU TSENG [2], MIN-SHIANG HWANG [1]

[1] Chair Professor, Department of Computer Science & Information Engineering Asia University, No. 500, Lioufeng Raod, Wufeng Shiang, Taichung, Taiwan, R.O.C.

[2] Department of Computer Science and Communication Engineering, Providence University, 200, Chung-Chi Rd., Taichung 43301, Taiwan R.O.C.

[3] Department of Computer Science and Engineering, National Chung Hsing University, 250, Kuo Kuang Rd., Taichung 402, Taiwan R.O.C.

E-MAIL: mshwang@asia.edu.tw, lytseng@pu.edu.tw, phd9406@cs.nchu.edu.tw

Abstract:

Enormous demands for recognizing complicated anatomical structures in medical images have been demanded on high quality of medical image such as each pixel expressed by 16-bit depth. Now, most of data hiding algorithms are still applied in 8-bit depth medical images. We proposed a histogram shifting method for image reversible data hiding testing on high bit depth medical images. Among image local block pixels, we exploit the high correlation for smooth surface of anatomical structure in medical images. Thus, we apply a different value for each block of pixels to produce a difference histogram to embed secret bits. During data embedding stage, the image blocks are divided into two categories due to two corresponding embedding strategies. Via an inverse histogram shifting mechanism, the original image will be accurately recovered after the hidden data extraction. Due to requirements of medical images for data hiding, we proposed six criteria: (1) Well-suited for high quality medical images (2) Without salt-and-pepper (3) Applicable to medical image with smooth surface (4) Well-suited sparse

histogram of intensity levels (5) Free location map (6) Ability of adjusting data embedding capacity, PSNR and Inter-Slice PSNR. We proposed a data hiding methods satisfying above 6 criteria.

Keywords:

reversible data embedding, histogram, difference expansion, medical image, criteria.

1. Introduction

Recently, most hospitals have already established the electronic medical information to make healthcare better, safer, and more efficient. Over the Internet, digitized medical information is very convenient to transmit among patients, medical professionals, health care providers, and institutes of medicine. However, many risks are more and more increasing such as illegal accessing and unauthorized tampering. Therefore, data hiding plays an important role in information security such as authentication, fingerprinting, copy control, security, and covert communication. Depending on the relationship between the embedded message and the cover image, data hiding techniques are divided into two categories: steganographic applications and digital watermarking. Applications of steganographic are no relationship to the cover image used for communication. The cover image means nothing to the sender except masking the secret message. Digital watermarking has a close relationship to the cover image such as adding the cover image caption, author signature, and authentication code in it.

According to permanent distortion of the cover image, digital watermarking are divided into irreversible data hiding and reversible data hiding [23][24]. Because of permanent distortion of the cover image, the original images cannot restore from stego-images Thus, irreversible data hiding techniques are hard to satisfy many circumstances such as in the field of law enforcement, medical imaging systems, military imaging systems, remote sensing, and high precision systems in

scientific research.

Nowadays, reversible data hiding, which is also called lossless data hiding, has drawn much attention among researchers [12][23][33]. Reversible data hiding has complete blind restoration of the original data from stego-images after the hidden data retrieved. In general, reversible data hiding techniques can be classified into three groups by Feng et al. [5]: data compression [3], pixel-value difference expansion (DE) [21][23][35] scheme and histogram-based scheme [12].

DE is one kind of integer wavelet transform proposed by Tian [30]. In order to realize a high-capacity and low-distortion reversible watermarking, Tian examined the redundancy in digital images by expanding the difference between the two neighboring pixel pairs to achieve a high-capacity and low-distortion reversible watermarking. By the generalized DE method, Alatter [1] applied Tian's scheme to hide several bits in the DE of vectors of adjacent pixels. Later on, Kim et al. [17] improved DE method to reduce the size of the location map. Further, Lin et al. proposed a DE scheme to remove the location map completely. In order to improve overflow map, Hu et al. [13] proposed a new DE algorithm.

Histogram shifting is another technique applied in reversible watermarking schemes. Vleeschouwer et al. [32] attempted to achieve reversibility by Circular interpretation of bijective transformations. Ni et al. [23] utilized a zero and a peak point of image histogram to embed messages. Luo et al. [19] exploits the high correlation among image block pixels to produce a difference histogram and embedded secret data by a multi-level histogram shifting mechanism.

In 2003, De Vleeschouwer et al. [32] proposed a robust lossless data hiding technique against a high-quality JPEG compression based on the modulo-256 addition. Unfortunately, applying the modulo-256 addition method will produce salt-and-pepper noise. Therefore, many papers [24] proposed a robust (or semi-fragile) lossless data hiding technique to overcome this drawback.

With the development of electronic medical information and the network technique, data hiding plays an important role for medical images. Until now, many algorithms [12][15][20] have been proposed. Most of them were applied in 8-bit depth medical image expressing intensity 0~255. Now, high quality medical devices are applied for improving the detection rate of diseases and treating at the early stage. A vast amount of demands for recognizing complicated anatomical structures in images have been required on high quality of medical image with 16-bit depth. Because of 16-bit depth with intensity 65,536 discrete levels and the smooth surface of anatomical structures required, it is becoming more and more difficult to find duplicate intensities embedding secret bits in embedding algorithms.

We develop a novel reversible data embedding scheme testing on 16-bit depth with dicom medical image. This scheme proposes 6 criteria well-suitable for requirements of medical images. The detail will be described in the following. This paper is organized as follows: Section 2 describes the criteria of reversible data hiding. Section 3, we present our method. Section 4 presents the experimental results. And finally in section 5 is conclusion and discussion.

2. The criteria of reversible data hiding

In general, the quality of a reversible data hiding is measured by payload capacity limit, visual quality, and complexity. However, high resolution medical images are different from low resolution medical images ex. 8-bit depth image. We divide the criteria of reversible data hiding into traditional criteria of reversible data hiding and the criteria of reversible data hiding in medical image described as follows.

2.1 Traditional criteria of reversible data hiding

The basic requirement of data hiding is low quality degradation on the image after data embedding. In order to measure the quality of a reversible data embedding, Tian [30] provided 3 criteria: (1)

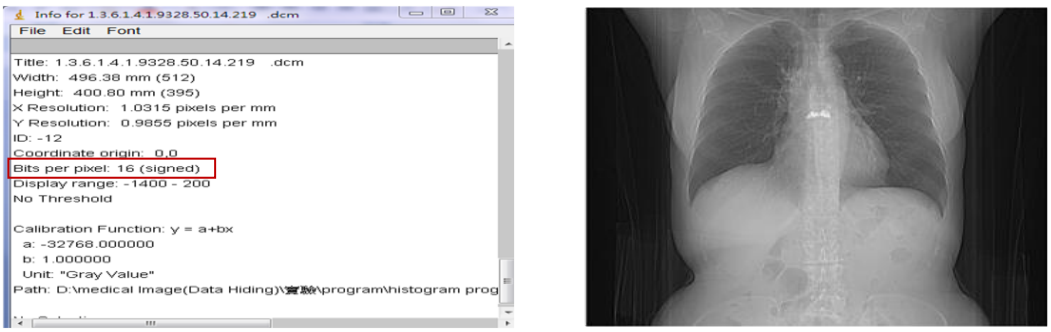

Figure 1. High quality medical images with 16-bit depth image from National Cancer Image Archive.

payload capacity limit (2) visual quality (3) complexity. We describe detail as follows:

(1) Payload capacity limit

The maximum amount of secret bits can be embedded to cover images with acceptable visual quality.

(2) Visual quality

The difference between the cover image and the stego-image is low degree of distortion. The PSNR is most commonly adapted to measure the quality of reconstruction of lossless data hiding.

(3) Complexity

The complexity is a method to measure efficiency of a data hiding algorithm. In general, complexity is analyzed by quantifying the amount of resources needed such as time and storage.

2.2. The criteria of reversible data hiding in medical image

Many medical images are a volume structure constructed by a series of images slices. Modern medical devices produce high quality medical images for detecting diseases. Therefore, more criteria are needed to measure high quality medical images for identifying complicated anatomical structures. We proposed 6 criteria to measure data hiding algorithms such as well-suited for high quality medical images, applicable to medical images with smooth surface, without salt-and-pepper, ability of

adjusting data embedding capacity, PSNR and Inter-Slice PSNR, sparse histogram of intensity levels, and free location map. The detail demonstrated as follows:

(1) Well-suited for high quality medical images

In digitalized images, a certain number of bits is assigned to each pixel to represent its intensity. The number of bits, the bit depth, will determine the number of gray levels between the minimum and maximum intensities that the imaging devices are able to capture. High quality images have high resolution and high bit-depth up to 12 bits or more per pixel. If the bit depth is not sufficient, the images will be a loss of gray-scale resolution [10][26]. In High-Resolution Computed Tomography (HRCT), CT images with a higher resolution and bit-depth can demonstrate subtle anatomical structures such as tissue characterization to detect diseases [34][38]. In other words, HRCT can get higher contrast CT data. Nowadays, enormous demands for recognizing complicated anatomical structures in medical images have been required on high quality of medical images [26] such as each pixels expressed by 16-bit depth as shown in Figure 1. A 16-bit depth image can handle 65,536 discrete levels of information instead of the 256 levels achieved by 8-bit image. In Figure 2, 8-bit images express intensity 255 as most of light anatomical structures in medical images. However, 16-bit depth image demonstrates the light part of anatomical structures as different intensity. In general, medical image have background of the images (or called None ROI) [6] which does not contribute to the diagnosis. Because high bit-depth medical images are detail-rich images, ROI area utilizes more intensity to presented anatomical structures for disease diagnosis. Some schemes are hard to embed secrets to ROI area. For instance, the schemes search for continuous duplicate values to hide secrets. Thus, most of secret bits will be embedded in None ROI area. Unfortunately, there is a copy attack [6] in these kinds of schemes. If a data hiding scheme is well-suited for high quality medical images, the embedded secret bits will distribute to whole images with copy attack avoidance.

(a) Dicom image (DCM) with 16-bit depth

263	276	338	151	151	180	200	145	140	115
333	327	397	212	217	229	289	207	164	160
295	320	305	276	244	312	349	270	202	171
264	330	271	342	313	328	378	309	263	202
257	301	305	345	321	304	302	269	316	224
227	256	305	329	268	205	239	223	203	152
224	218	263	274	238	191	171	153	133	64
171	133	178	195	144	151	154	137	95	94
107	62	102	118	86	111	129	104	123	153
83	47	79	121	114	110	123	113	126	147

(b) Intensities of ROI.

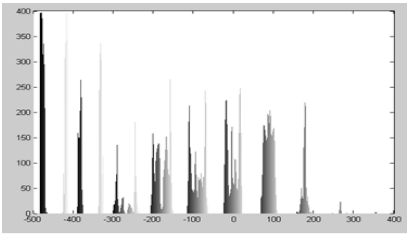

(c) Histogram range -492~397

(d) Bitmap (Bmp) image with 8-bit depth

255	255	255	248	248	253	255	247	246	242
255	255	255	255	255	255	255	255	250	249
255	255	255	255	255	255	255	255	255	251
255	255	255	255	255	255	255	255	255	255
255	255	255	255	255	255	255	255	255	255
255	255	255	255	255	255	255	255	255	248
255	255	255	255	255	254	251	248	245	234
251	245	252	255	247	248	248	246	239	239
241	234	240	243	238	242	244	240	244	248
237	231	236	243	242	241	244	242	244	247

(e) Intensities of ROI.

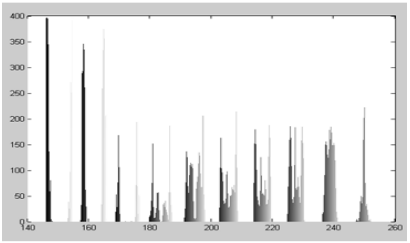

(f) Histogram range 145~255

Figure 2. 16-bit depth dicom image compare with 8-bit depth bitmap image

(2) Without salt-and-pepper

Salt and pepper noise is one kind of noise typically seen on images presented by white and black pixels. In other words, the histogram for the salt-and-pepper has an extra peak at the white end of the spectrum since the noise components were pure black and white [11] as shown in Figure 3.

From the position of salt-and-pepper, the illegal attackers can easily get the information to revise the stego-image.

(3) Applicable to medical image with smooth surface

In medical images, volume structure is an important feature to record the complexity and variability of anatomical shape. A volume structure is assembled by a series of medical image slices from image scanner. For instance, a complete scan of an average patient's lung cavity produces approximately 500 isotropic CT images [22][36]. Furthermore, each slice of images can

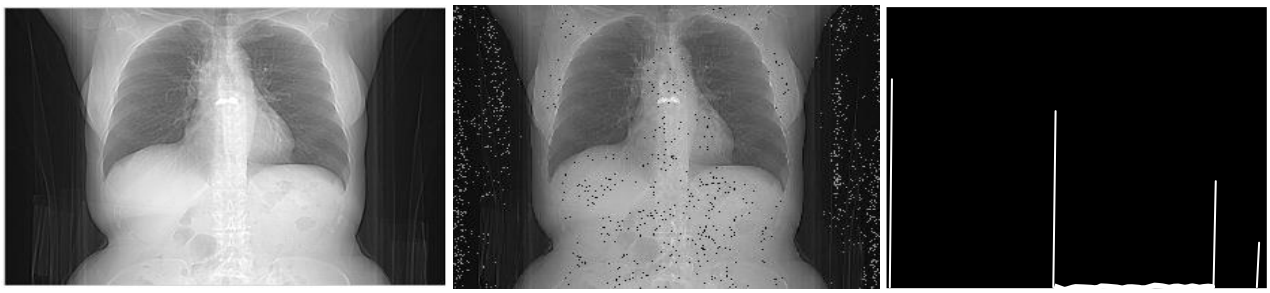

(a) Original Image (b) Stego-Image with Salt-and-Pepper (c) histogram of Salt-and-Pepper

Figure 3. Salt-and-Pepper noise on medical image

also be reconstructed 3D model to detect anatomical structures such as nodule, fissure, and trachea [2]. By geometric algorithm, surfaces of anatomical structures will be detected by smooth implicit functions [37]. Therefore, it is important for data hiding scheme to preserve smooth surface in medical images.

In order to measure smooth surface in volume of medical images, we define a formula to compare original slices with stego slices by the average difference intensity described as follows.

$$P(i,j) = avg\ (|p - p_L| + |p - p_R| + |p - p_U| + |p - p_D| + |p - p_{next}|) \quad (1)$$

Where i = 1,…,W, j = 1,…,H. p_L, p_R, p_U and p_D are left, right, up, down pixel of p respectively. p_{next} is the position p located on the next slice. We compute the average difference intensity of each pixel $p_{\text{cover}}(i,j)$ and $p_{stego}(i,j)$ for cover image and stego image respectively. Then we construct $p_{\text{cover}}(i,j)$ as a new image name as $C_{difference}$. And construct $p_{stego}(i,j)$ as a new image called $S_{difference}$. The PSNR of $C_{difference}$ and $S_{difference}$ image defines as follows.

$$Inter-Slice\ \ PSNR = 10\log_{10}\frac{(\text{Im}age\ \ Bit\ \ depth\ )^2}{MSE_{Inter-Slice}} \quad (2)$$

$$MSE_{Inter-Slice} = \frac{1}{m \times n}\sum_{i=1}^{m}\sum_{j=1}^{n}(C_{difference}(i,j) - S_{difference}(i,j))^2 \quad (3)$$

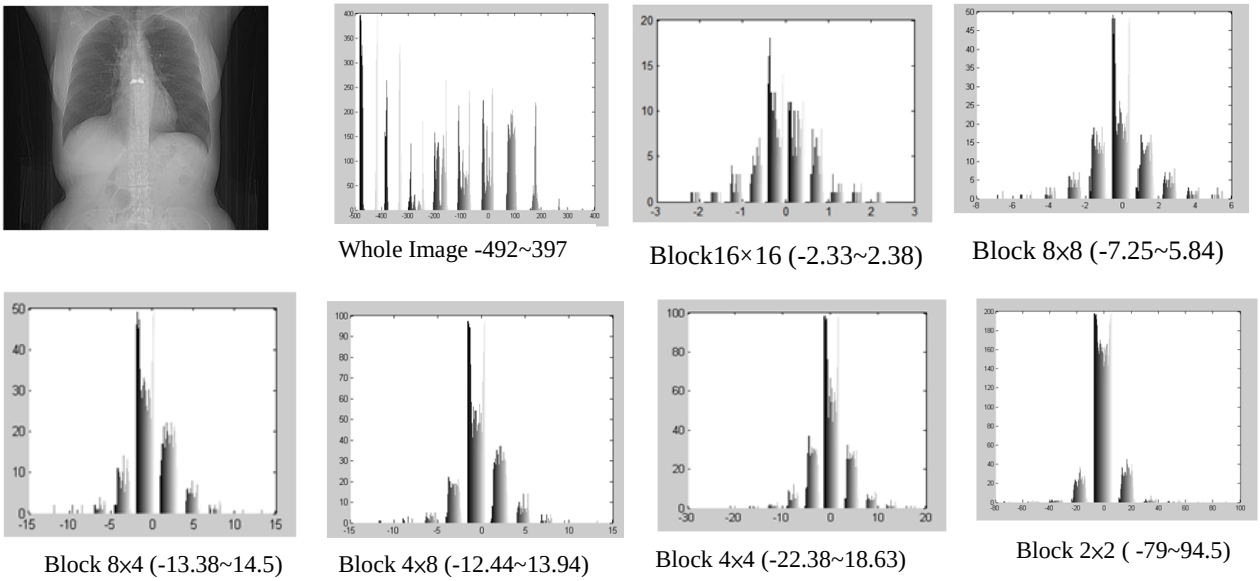

Figure 4. The histogram of difference values by different block sizes

Where m and n are the width and height of the $C_{difference}$ and $S_{difference}$. All Inter-Slice PSNR of volume medical images can present the quality of smooth surface.

(4) Well-suited sparse histogram of intensity levels

In high bit-depth (up to 12 bits per pixel or more) of medical images modalities such as CR, CT, MR, and US, the images have sparse histogram of intensity levels [27][28][29]. In other words, the image intensities are quantized to a number of levels on the wider range to make viewing images easier. Thus, the brightest actual level gets closer to the brightest nominally possible. The numeric values of originally consecutive quantization levels result in consecutive integers, i.e. less continuous duplicate value. There are many data hiding proposed by recording continuous duplicate value to embed data. Due to medical images with 16-bit depth, more intensity demonstrates different anatomical structures producing duplicate values rarely.

(5) Free location map

In order to reversible data hiding, some reversible data hiding methods must embed partial image data [12] or hiding an image-dependent location map for image restoration [31]. Some methods

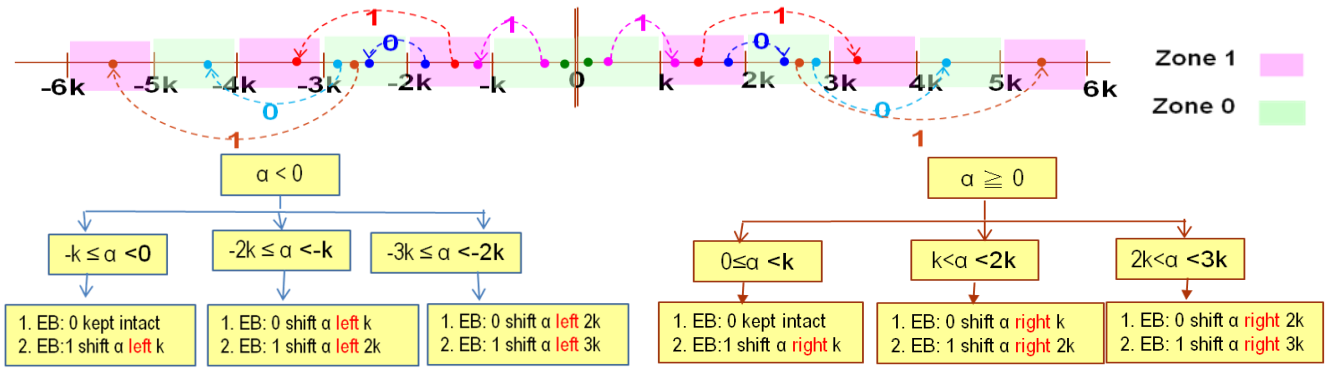

Figure 5.The strategy of data embedding where k is threshold and α is difference value.

[16][17][19] need to produce location map or coefficient map to remember the embedding to solve overflow and underflow problems. However, those methods not only consume location map storage but also require computation costs highly for hidden data extraction. For huge image database or video database, location map also prevent real time data extraction for video sequences [14]. Therefore, it is important to develop location map-free methods [7][8] for data hiding.

(6) Ability of adjusting data embedding capacity, PSNR, and Inter-Slice PSNR

We can adjust block size, partition level, number of embedding bits to handle capacity, PSNR., and Inter-Slice PSNR. Large block size will improve PSNR and decrease capacities. Conversely, small block size can increase capacities and reduce PSNR. By experiment shown in Session 4, capacity and PSNR is higher than those of partition level 3.When the embedding bits are increased, PSNR will reduce and capacity is going to increase. Inter-Slice PSNR will decrease when block size is small. In order to meet the requirements of medical images, we can apply the proper block size, partition level, number of embedding bits to process data hiding.

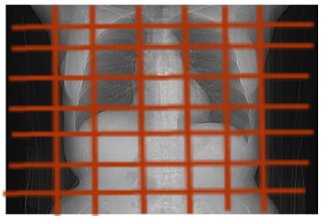

(a) Image None overlaying blocks partition with 16-bit depth

7	12	11	6	6	11	12	8
5	9	9	5	6	11	12	9
2	5	5	4	5	10	12	10
0	1	2	3	5	9	11	11
1	0	1	3	5	6	9	11
4	1	1	4	5	4	6	9
8	4	3	6	6	2	3	7
11	5	4	7	6	1	1	6

(b) pixel values from one of block

+	-	+	-	+	-	+	-
-	+	-	+	-	+	-	+
+	-	+	-	+	-	+	-
-	+	-	+	-	+	-	+
+	-	+	-	+	-	+	-
-	+	-	+	-	+	-	+
+	-	+	-	+	-	+	-
-	+	-	+	-	+	-	+

(c) Difference pair pattern.

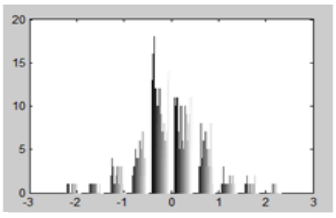

(d) Histogram of all difference values range from -2.33 to 2.38

Figure 6.Compute difference value for each block

3. A Reversible Image Data Hiding Algorithm

Due to the smooth surface of anatomical structures in medical images, difference values of local block pixels have a high correlation, and expected to be very close to zero. We proposed histogram shifting model utilizing the statistics of difference value to decide the optimal threshold k for embedding secret bits. Depending on difference value of each block, data embedding strategy is divided into two categories: negative and positive values. There are 8 steps at data embedding stage. The details are demonstrated in Figure 7, which shows the flowcharts of the embedding process.

3.1. Data Embedding

Data embedding strategy applies optimal threshold k to embed secret bits by a shift quantity nk ($n \geq 0$). The main idea for bit embedding is that the difference value α is kept within a specified range of thresholds nk and -nk to embed bits “1” or “0”. Based on the difference value α, data embedding strategy is separated into two categories: positive difference values ($\alpha \geq 0$) and negative

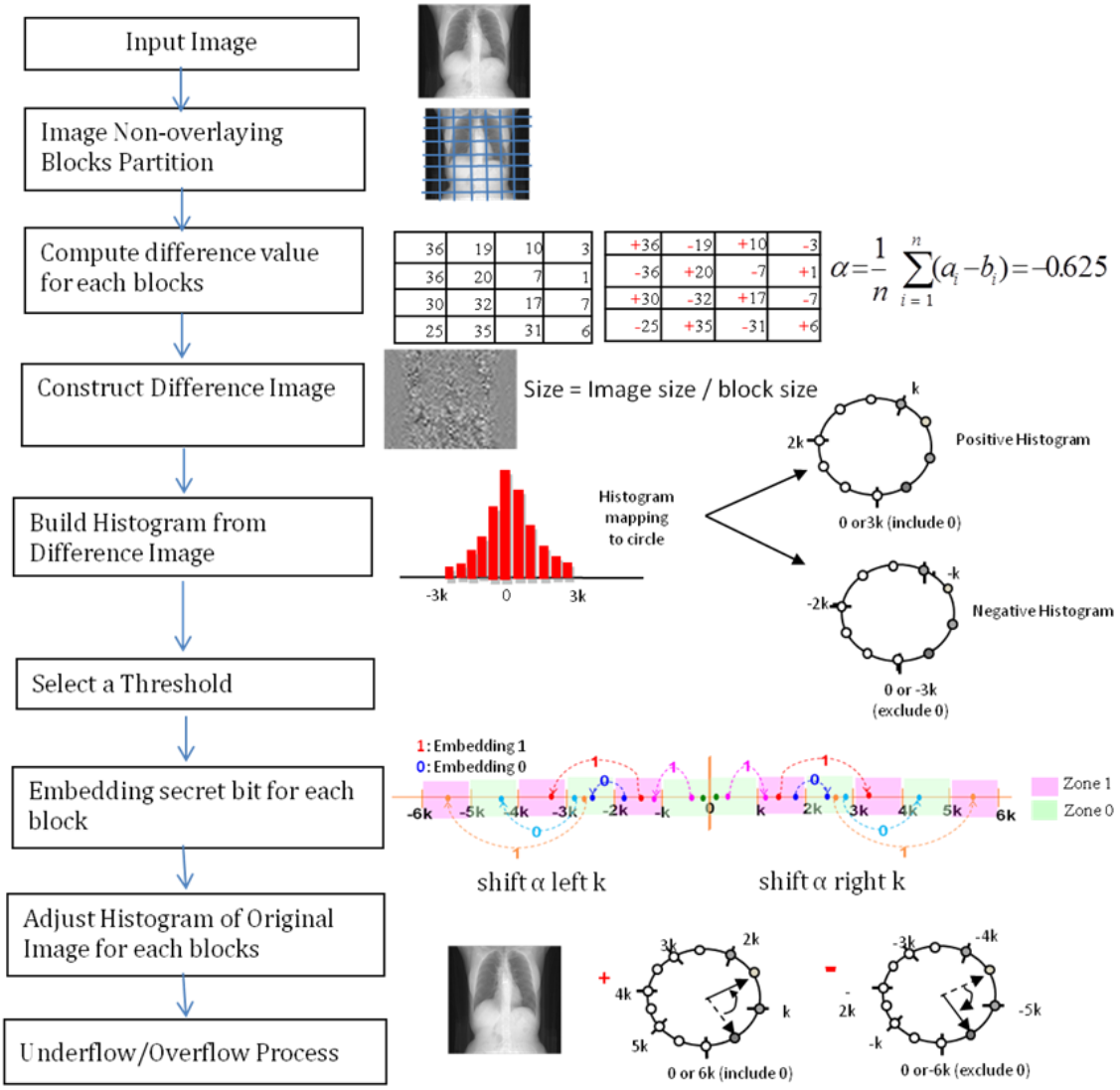

Figure 7. The flowcharts of the embedding process.

difference value ($\alpha < 0$). For all non-overlaying blocks, the statistics of difference value of each block is divided into zone 0 and zone 1, which embed "0" and "1" respectively. The strategy of data embedding is demonstrated in Figure 5. The embedding process is described as follows:

Step 1: Image by Non-overlaying Blocks Partition

In the technique suggested in the Ni method [23] , the image I with size W × H is divided into a set of u × v blocks where u and v are even.

Step2: Computation of difference value for each of blocks

In general, pixels of a block are highly correlated and exhibit strong spatial redundancy in local blocks of the image. Therefore, it is possible to create a free space for embedding extra information by transforming the image. Suppose each block of difference pair pattern M(i, j) is a $W_b \times H_b$ binary image and divided into A and B zone. The definition describes as follows.

$$Zone\ A = \begin{cases} M(2i-1,\ 2j-1) = 1 \\ M(2i,\ 2j) = 1 \end{cases} \quad (4)$$

$$Zone\ B = \begin{cases} M(2i-1,\ 2j) = -1 \\ M(2i,\ 2j-1) = -1 \end{cases} \quad (5)$$

Where i = 1, ..., $W_b/2$, j = 1, ..., $H_b/2$. Both W_b and H_b are even.

In Figure 4, the histogram of difference values will be close to zero. Considering image block size 8 × 8, the block is equally divided into two sets of pixels, i.e. zones A and B. Zone A are marked by "+" and Zone B marked by "-" as shown in Figure 6. Let a_i is all pixels of marked by "+" and b_i is all pixels of marked by "-". The difference value α is defined as the arithmetic average by pixel pairs grayscale values within the block. Therefore, two neighboring pixels are selected and further marked by "+" and "-" to calculate difference value α. The formula of difference value α is describes as below.

$$\alpha = \frac{1}{n}\sum_{i=1}^{n}(a_i - b_i) \quad (6)$$

Where n is the number of pixel pairs. For instance, a given 8 × 8 image block will produce 32 pixel pairs. The difference value α will be obtained -0.0625 by the formula (6). The histogram of difference values will be concentrated on zeros and distributed between -2.33 to 2.38.

Step3: Construction of difference image

When difference values in each block are produced, the total number of difference values will be used to construct a difference image. For a (u × v) image, the size of the difference image can be computed as:

$$\text{Size of difference image} = \left\lfloor \frac{W}{u} \right\rfloor \times \left\lfloor \frac{H}{v} \right\rfloor \quad (7)$$

where W × H is the size of Image and u × v is the size of block. Both u and v are also even.

Step 4: Building histogram from difference image

When the difference value α is produced in each block, the total number of differences N_d are applied to generate histogram statistics as

$$N_d = \left\lfloor \frac{W}{u} \right\rfloor \times \left\lfloor \frac{H}{v} \right\rfloor \quad (8)$$

Where W × H is the total number of image, u × v is the total number of blocks. Both of u and v are even. Obviously, a smaller block size partition corresponds to a larger N_d.

Step 5: Selecting threshold

We compute a positive optimal threshold from positive blocks of difference images. In the same way, a negative optimal threshold will be computed from negative blocks of difference images. The formula is described as follows:

(1) Difference α ≥ 0

$$k_{P\_h} = \left\lceil (\alpha_{\max\_P} - \alpha_{zero} + 1) / PartitionLevel \right\rceil \quad (9)$$

$$k = k_{P\_h} + \left| \bmod(k_{P\_h}, 2) \right| \quad (10)$$

Where α_{max_P} is maximum difference values from the whole positive part and α_{zero} is 0

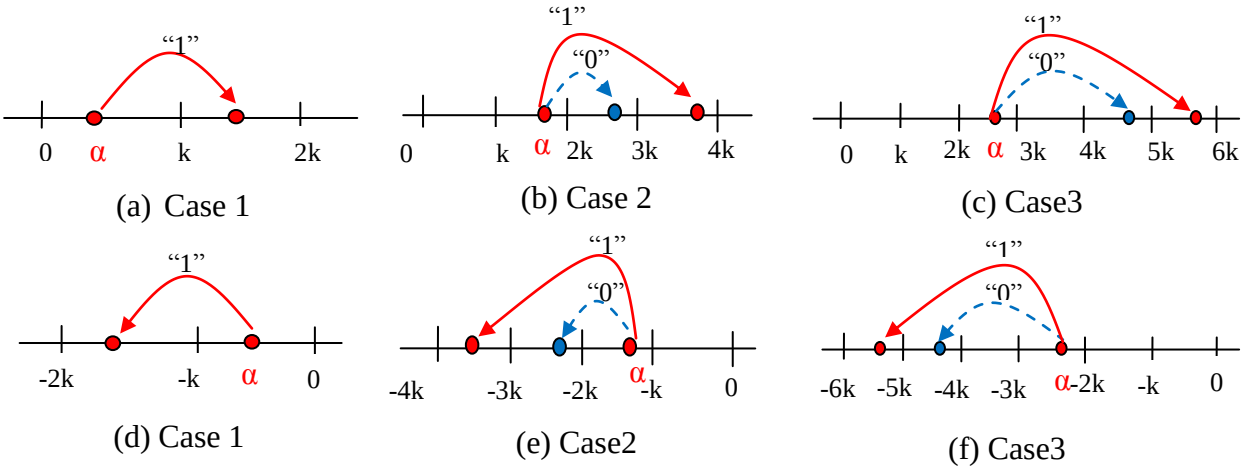

Figure 8. Block histogram for category 1 shown in (a)(b)(c) and category 2 shown in (d)(e)(f).

for the center of the coordinate. Partition Level is the parameter of partition number. For instance, the image of difference values are -2.33, -2, -2.3, 1.2, 2.38, and partition level is set to 3. α_{max_P} is 2.38 and α_{zero_P} is 0. Thus, the optimal threshold k will be obtained 2 shown as follow.

$$k_{P\_h} = \lceil (2.38 - 0 + 1)/3 \rceil = 2$$

$$k = 2 + \left| \mathrm{mod}(2,\ 2) \right| = 2$$

(2) Difference $\alpha < 0$

$$k_{N\_h} = \left| (\alpha_{zero} - \alpha_{\min\_N} + 1)/PartitionLevel \right| \quad (11)$$

$$-k = (\ k_{N\_h} + \left| \mathrm{mod}(k_{N\_h}, 2) \right|\ ) * -1 \quad (12)$$

Where α_{max_N} is maximum of difference values from the whole negative part. For example, the image of difference values are -2.33, -2, -2.3, 1.2, 2.38, and partition level is set to 3. α_{zero} is 0 and α_{min_N} is -2.33. Thus, the optimal threshold k will be obtained 2 demonstrated as follow.

$$k_{N\_h} = \lceil (0 - (-2.33) + 1)/3 \rceil = 2$$

$$-k = (2 + \lceil \mathrm{mod}(2,2) \rceil\ ) = -2$$

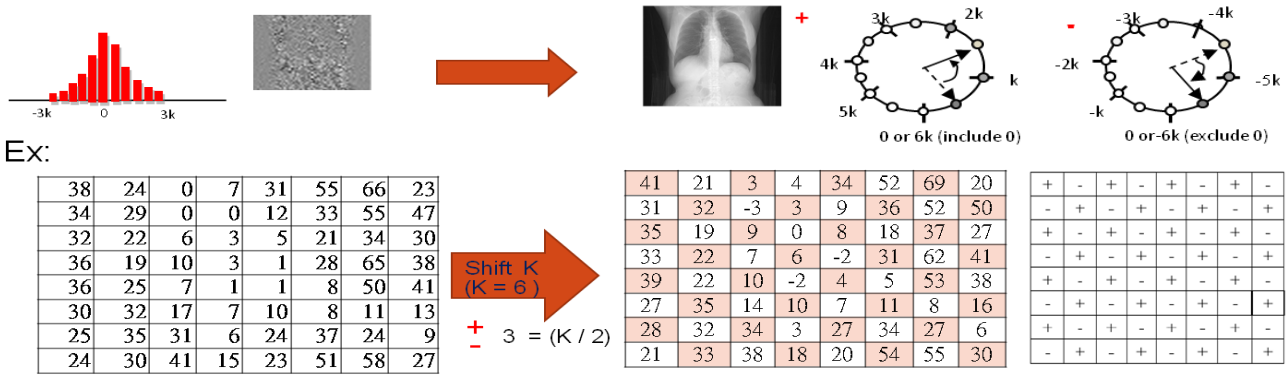

Figure 9 Adjust histogram of original image for each blocks

Step 6: Embedding secret bits for each of blocks by histogram shifting

This step is the important operation of data embedding, and different values α for each block are tackled with different shifting strategies. For simplicity, we take the example of PL (Partition Level) = 3 and 8 × 8 block partition as shown in Figure 5. These embedding strategies are based on the difference value α and divided into two categories: positive and negative values as shown in Figure 5 and Figure 8.

Category 1: The difference value α is positive value, $\alpha \geq 0$.

In this category, the difference value α is always positive. For simplicity, the partition level (PL) is set to 3. Therefore, three cases are considered in the following.

Case 1: $0 \leq \alpha \leq k$

In this case, the difference value α is located between threshold 0 and k. If embedding bit is "1", the histogram of the block is shifted to right with distance k. If embedding bit is "0", the block keeps intact.

Case 2: $k \leq \alpha \leq 2k$

In this case, the difference value α is located between threshold k and 2k. If

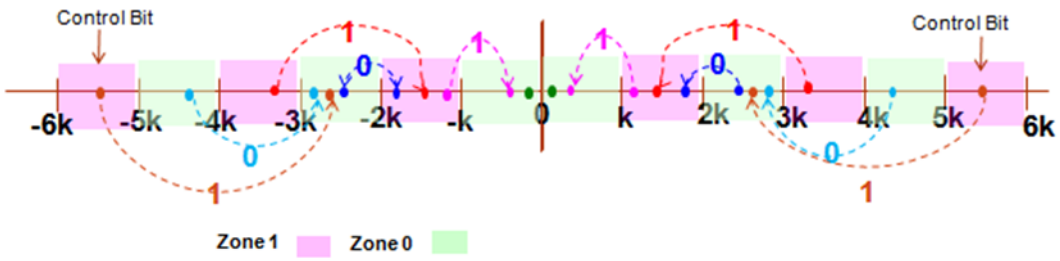

Figure 10. The strategy of data extraction where k is an optimal threshold with partition level 3.

embedding bit is "1", the histogram of the block is shifted right to 2k. If the embedding bit is "0", the histogram of the block is shifted right to k.

Case 3: $2k \leq \alpha \leq 3k$

In this case, the difference value α is located between threshold 2k and 3k. If embedding bit is "1", the histogram of the block is shifted right to 3k. If the embedding bit is "0", the histogram of the block is shifted right to 2k.

Category 2: The difference value α is negative value, $\alpha < 0$.

In this category, we consider the difference value α is always negative. There are three cases demonstrated as the following.

Case 1: $-k \leq \alpha \leq 0$

In this case, the difference value α is located between threshold -k and 0. If embedding bits is "1", the histogram of the block is shifted left to k. if embedding bit is "0", the block keeps intact.

Case 2: $-2k \leq \alpha \leq -k$

In this case, the difference value α is located between threshold -2k and –k. If embedding bit is "1", the histogram of the block is shifted left to 2k. If the embedding bit is "0", the histogram of the block is shifted left to k.

Case 3: $-3k \leq \alpha \leq -2k$

In this case, the difference value α is located between threshold -3k and -2k. If embedding bit is “1”, the histogram of the block is shifted left to 3k. If the embedding bit is “0”, the histogram of the block is shifted left to 2k.

The previous conditions of two categories cover all situations that a block may encounter. Because the pixel grayscale values in a local block are often highly correlated, the optimal threshold k will not be changed dramatically on sign 16-bit depth in medical image. Apparently, the detailed description of the bit-embedding procedure demonstrates that the modified pixel grayscale value is still on range of image, and hence no overflow/underflow will take place. The detail is described in Step 8. For improving PSNR in small block size, we also can set a threshold of histogram to embed secrets described in section 2.2(6).

Step 7: Adjusting histogram of original image for each blocks

The optimal threshold k divided by 2 is known as half optimal threshold. Add half optimal threshold to “+” part. At the same time, subtract half optimal threshold from “-” part. If the optimal threshold is 6, the element of 38 will be a member of “+”. Thus 38 plus half optimal threshold is equal to 41. Applying the same process, the element of 24 is a member of “-”. Therefore, 24 minus half optimal threshold is equal to 21, demonstrated as Figure 9.

Step 8: Overflow/Underflow process

In general, the store format of medical image slices can be divided two categories: sing bit and unsign bit. Therefore, both of them have the different ways to process overflow/underflow problem. At first, we compute the utilization rate as follows.

$$intensity\ rate\ = \frac{the\ \ range\ \ of\ \ inttensity}{2^{bit\_depth}} \quad (13)$$

$$underflow/overflow\ rate\ = \frac{value\ \ of\ \ underflow\ \ /overflow}{2^{bit\_depth}} \quad (14)$$

$$The\ Utilization\ Rate = abs(\ intensity\ rate) + abs(underflow/overflow\ rate) \quad (15)$$

Next step is adjust image histogram to prevent overflow/underflow problem. Because of underflow/overflow rate is generally very low in high bit-depth medical images, unsing bit images have underflow problem and sign bit images have no overflow/underflow problem. Therefore, we adjust the histogram of stego image to right shift with underflow distance in unsign bit image when concentrate rate is less than 1 without location map. For instance unsign 16-bit depth in TABLE VI, the slice No.000000.dcm has the intensity rate 0.0141 (max intensity 923 min intensity 0) and underflow/overflow rate -0.000061(-4/2^{16}). Thus, the Utilization Rate is 0.0140. The 16-bit depth images have enough intensity to solve underflow problem apparently. Therefore, we shift histogram leftward 4 for underflow.

3.2. Data Extraction

Data extraction process will extract secret message correctly and can reverse the marked image back to the original without any distortions. There are some parameters for data extraction such as block size, partition level, number of embedding bits, and the shift histogram value for underflow/overflow. At the first step, the image shift back histogram for overflow/underflow. Similar to data embedding process, the second step is image

TABLE I. The Range of Difference Values and PSNR with Different Block Size

Block Size	1.3.6.1.4.1.9328.50.14.219.dcm				1.3.6.1.4.1.9328.50.14.320.dcm				1.3.6.1.4.1.9328.50.14.160.dcm			
	Min Difference	Max Difference	PSNR	Underflow/ Overflow	Min Difference	Max Difference	PSNR	Underflow/ Overflow	Min Difference	Max Difference	PSNR	Underflow/ Overflow
16×16	2.33	2.38	99.34	No	-3.2	4.8	98.55	No	-2.46	2.84	99.13	No
8 × 8	7.25	5.84	97.51	No	-11.44	8.09	90.87	No	-7.28	6.81	92.92	No
8 × 4	-13.38	14.5	92.58	No	-13.88	18.38	88.03	No	-11.56	10.75	90.5	No
4 × 8	-12.44	13.94	92.51	No	-19.13	17.63	87.11	No	-12	12.38	89.35	No
4 × 4	-22.38	18.63	89.07	No	-22	30.88	84.72	No	-23.75	22.25	85.82	No
2 × 2	-79	94.5	78.49	No	-103	149.5	72.38	No	-71.5	129.5	74.23	No

non-overlaying blocks partition with block size 8 × 8, 4 × 4, 2 × 2 and so on. Then, compute the difference value α from each block by the formula (6). According to all of difference value α, we construct difference image and build histogram for extraction. Next step, the optimal threshold is computed by the following formula:

$$k_{P\_h} = \left| (\alpha_{\max\_P} - \alpha_{zero} + 1) / PartitionLevel * 2 \right| \quad (16)$$

$$k = k_{P\_h} + \left| \bmod(k_{P\_h},\ 2) \right| \quad (17)$$

Since both minimum and maximum control bits are embedded, the optimal threshold k will be recovered correctly. According to all of difference value and optimal threshold k, each of block difference values is tackled with different shifting strategies as shown in Figure 10. If difference value α fall on the zone "0", the extract bit "0" will be extracted and the difference value α is shifted toward left. If difference value α fall on the zone "1", the extract bit "1" will be extracted and the difference value α is shifted toward left. For instance, if a block difference value is located in 5k~6k belonging to zone "1", the secret bit "1" will be extracted and the difference value will

TABLE II . Test results for a 395×512×16 Grayscale Medical Image with partition as 3, 4

Image	Block size	Capacity	Partition Level = 3	Partition Level = 4
			PSNR	PSNR
Dcm 395×512 (16bits)	16×16	768	99.21	99.34
	8×8	3,136	93	97.51
	8×4	6,272	89.51	92.58
	4×8	6,272	89.49	92.51
	4×4	12,544	86.78	89.07
	2×2	50,432	75.69	78.49
	2×1	100,864	70.32	73.13
	1×2	101,120	65.1	67.68

TABLE III. Test results for a 395×512×16 Grayscale Medical Image with secret 1-bit and 2-bit

Image	Secret 1-bit				Secret 2-bit		
	Partition Level = 4				Partition Level = 4		
	Block size	Capacity		PSNR	Capacity		PSNR
		(bits)	(bpp)		(bits)	(bpp)	
Dcm 395×512 (16bits)	16×16	766	0.004	99.3	1,532	0.008	90.45
	8×8	3,134	0.016	97.5	6,268	0.031	86.1
	8×4	6,270	0.031	92.6	12,540	0.062	83.72
	4×8	6,270	0.031	92.5	12,540	0.062	83.72
	4×4	12,542	0.062	89.1	25,084	0.124	80.18
	2×2	50,430	0.249	78.5	100,858	0.499	69.65
	2×1	100,862	0.499	73.1	201,724	0.997	64.17
	1×2	101,118	0.500	67.7	202,236	1.000	58.96

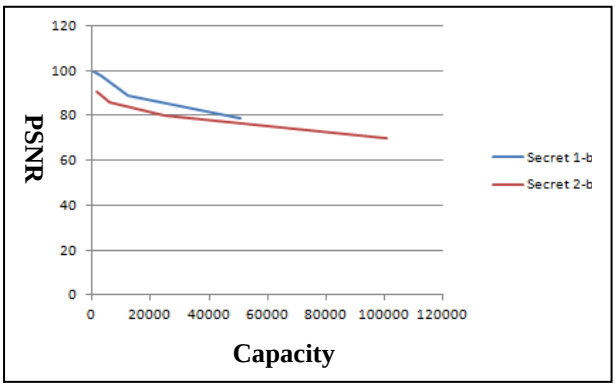

(a) The more capacity increases, the more PSNR decreases.

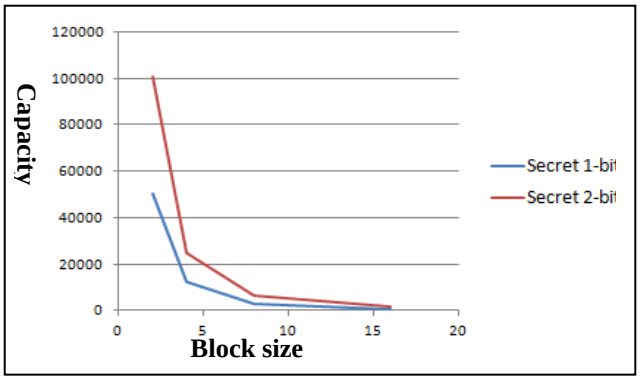

(b) The smaller block size, the higher amount of capacity. At the block size 5, the amounts of capacity of secret 2-bit will be increased dramatically.

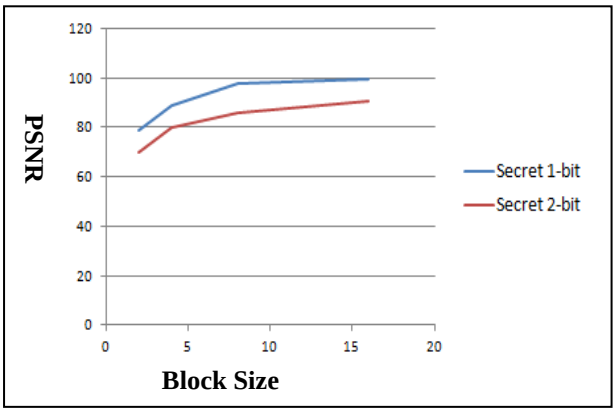

(c) The lower block size, the lower PSNR.

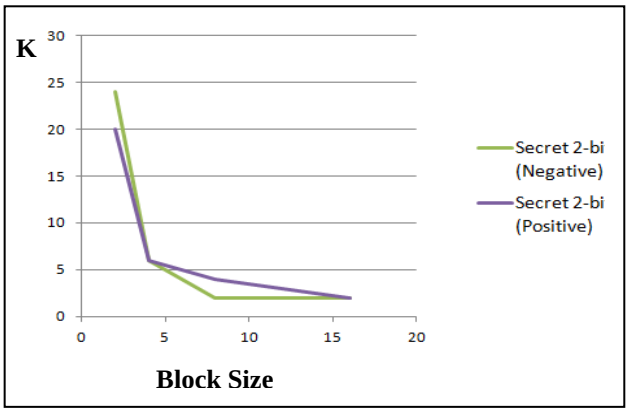

(d) The higher block size, the lower optimal threshold **K.**

Figure 11. The relation of PSNR, Capacity, optimal threshold k, and Block size.

be shifted back toward 2k~3k with distance 3k. The difference α of each block is not parameter for embedding phase and extraction phase. In other words, difference α will produce different value in cover image and stego-image. According to the strategy of data extraction in Figure 10, we can extract the original image and secret bits correctly.

4. Experimental Results

Our scheme has successfully applied to high quality medical images of the patient slice with standard dicom format medical image DICOM (Digital Imaging and Communications in Medicine) from the

TABLE IV. The results for sign 16-bit Grayscale Medical Image with secret 2-bit and partitioned as 4

Image Name from the National Cancer Imaging Archive	Image Size	2 × 2				4 × 4			
		Capacity	bpp	Overflow /Underflow	PSNR	Capacity	bpp	PSNR	Overflow /Underflow
1.3.6.1.4.1.9328.50.14.159.dcm	395 × 512	100,860	0.49871	No	66.21	25,084	0.12403	73.63	No
1.3.6.1.4.1.9328.50.14.1207.dcm	429 × 512	109,564	0.49882	No	68.23	27,388	0.12469	75.06	No
1.3.6.1.4.1.9328.50.14.1210.dcm	429 × 512	109,564	0.49882	No	71.72	27,388	0.12469	81.59	No
1.3.6.1.4.1.9328.50.14.1278.dcm	444 × 512	113,660	0.49998	No	70.51	28,412	0.12498	80.64	No
1.3.6.1.4.1.9328.50.14.1280.dcm	444 × 512	113,660	0.49998	No	63.17	28,412	0.12498	71.18	No
1.3.6.1.4.1.9328.50.14.157.dcm	395 × 512	100,860	0.49871	No	69.06	25,084	0.12403	79.09	No
1.3.6.1.4.1.9328.50.14.1141.dcm	458 × 512	117,244	0.49998	No	72.77	29,180	0.12444	80.88	No
1.3.6.1.4.1.9328.50.14.160.dcm	444 × 512	113,660	0.49998	No	67.72	28,412	0.12498	79.16	No
1.3.6.1.4.1.9328.50.14.163.dcm	444 × 512	113,660	0.49998	No	65.06	28,412	0.12498	71.57	No
1.3.6.1.4.1.9328.50.14.1908.dcm	547 × 512	139,772	0.49907	No	60.06	34,812	0.12430	69.77	No
1.3.6.1.4.1.9328.50.14.1911.dcm	547 × 512	139,772	0.49907	No	64.42	34,812	0.12430	76.79	No
1.3.6.1.4.1.9328.50.14.2.dcm	350 × 512	89,596	0.49998	No	62.67	22,268	0.12426	71.52	No
1.3.6.1.4.1.9328.50.14.2084.dcm	424 × 512	108,540	0.49998	No	69.06	27,132	0.12498	80.06	No
1.3.6.1.4.1.9328.50.14.2087.dcm	424 × 512	108,540	0.49998	No	63.82	27,132	0.12498	71.13	No
1.3.6.1.4.1.9328.50.14.2143.dcm	454 × 512	116,220	0.49998	No	66.05	28,924	0.12443	73.07	No
1.3.6.1.4.1.9328.50.14.2146.dcm	454 × 512	116,220	0.49998	No	67.46	28,924	0.12443	78.13	No
1.3.6.1.4.1.9328.50.14.216.dcm	395 × 512	100,860	0.49871	No	64.79	25,084	0.12403	76.38	No
1.3.6.1.4.1.9328.50.14.57.dcm	523 × 512	133,628	0.49903	No	67.09	33,276	0.12427	73.35	No
1.3.6.1.4.1.9328.50.14.219.dcm	395 × 512	100,858	0.49870	No	69.65	25,084	0.12403	80.18	No
1.3.6.1.4.1.9328.50.14.2363.dcm	523 × 512	133,628	0.49903	No	65.92	33,276	0.12427	78.33	No
1.3.6.1.4.1.9328.50.14.2366.dcm	523 × 512	133,628	0.49903	No	59.70	33,276	0.12427	71.37	No
1.3.6.1.4.1.9328.50.14.2422.dcm	523 × 512	133,628	0.49903	No	61.28	33,276	0.12427	69.52	No
1.3.6.1.4.1.9328.50.14.2425.dcm	523 × 512	133,628	0.49903	No	58.52	33,276	0.12427	69.63	No
1.3.6.1.4.1.9328.50.14.2499.dcm	523 × 512	133,628	0.49903	No	62.20	33,276	0.12427	69.85	No
1.3.6.1.4.1.9328.50.14.2502.dcm	523 × 512	133,628	0.49903	No	65.28	33,276	0.12427	76.57	No
1.3.6.1.4.1.9328.50.14.320.dcm	414 × 512	105,980	0.49998	No	66.45	26,364	0.12438	78.64	No
1.3.6.1.4.1.9328.50.14.322.dcm	414 × 512	105,980	0.49998	No	61.46	26,364	0.12438	68.06	No
1.3.6.1.4.1.9328.50.14.323.dcm	463 × 512	118,268	0.49890	No	65.93	29,436	0.12417	77.04	No
1.3.6.1.4.1.9328.50.14.326.dcm	463 × 512	118,268	0.49890	No	56.67	29,436	0.12417	65.95	No
1.3.6.1.4.1.9328.50.14.442.dcm	395 × 512	100,860	0.49871	No	60.62	25,084	0.12403	67.92	No
1.3.6.1.4.1.9328.50.14.445.dcm	395 × 512	100,860	0.49871	No	66.54	25,084	0.12403	75.27	No
1.3.6.1.4.1.9328.50.14.54.dcm	523 × 512	133,628	0.49903	No	68.10	33,276	0.12427	79.97	No

National Cancer Imaging Archive [25]. We adopt MATLAB to implement our method and the program was run on a Notebook with 2.67 GHz processor and 4.0 GB RAM. On average, 8.75 seconds were required to embed secrete bits on a 444×512 CT slice. For measure experiments, the stego-images

was measured by PSNR (peak signal to noise ratio) and MSE (mean square error) defined as the following:

TABLE V. Test results for unsign 16-bit Grayscale Medical Image with secret 1-bit and partitioned as 3

Image Name	Image Size	Block Size	Capacity	bpp	PSNR	Overflow/ Underflow	Underflow (minimum value)
000000.dcm	256 × 256	16 × 16	155	0.00237	85.62489	Yes	-3
		8 × 8	970	0.01480	94.06471	Yes	-1
		8 × 4	1958	0.02988	89.33524	Yes	-2
		4 × 8	1995	0.03044	93.61658	Yes	-1
		4 × 4	3983	0.06078	83.49892	Yes	-4
		2 × 2	16307	0.24883	74.66973	Yes	-11

TABLE VI. The results for unsign 16-bit Grayscale Medical Image with secret 1-bit and partitioned as 3

Image Name from the National Cancer Imaging Archive	4 × 4						
	Image Size	Capacity	bpp	PSNR	Overflow/Underflow	Underflow (minimum value)	Inter-Slice PSNR
000000.dcm	256 × 256	3,983	0.06078	83.49892	Yes	-4	0.00000
000001.dcm		3,970	0.06058	85.40303	Yes	-3	54.75864
000002.dcm		4,036	0.06158	83.31771	Yes	-4	54.76623
000003.dcm		3,967	0.06053	81.53948	Yes	-5	54.21060
000004.dcm		3,952	0.06030	77.85192	Yes	-8	52.82697
000005.dcm		3,960	0.06042	78.82331	Yes	-7	52.20390
000006.dcm		4,036	0.06158	74.49475	Yes	-12	50.49584
000007.dcm		3,955	0.06035	77.76524	Yes	-8	50.41839
000008.dcm		3,976	0.06067	74.44366	Yes	-12	50.63647

$$PSNR = 10\log_{10}\frac{(\mathrm{Im}age\ Bit\ depth\ )^2}{MSE},\ and$$

$$MSE = \frac{1}{m \times n}\sum_{i=1}^{m}\sum_{j=1}^{n}(c_{ij} - \bar{c}_{ij})^2$$

Where image bit depth is 16. m and n are the width and height of the cover image and the stego-image. $c_{ij} and\ \bar{c}_{ij}$ are the intensities of the pixels located between cover and stego images. With different block size, PSNR will be decreased because the maximum and minimum of difference value have a larger distance shown in TABLE I. A collection of various block size experiments affects the capacity and PSNR shown in TABLE II. Large block size resulted in the embedding capacities of decreasing. However, small block size with more capacities will make PSNR reduce. For each block size and capacity, values of PSNR in partition level 4 is higher than those of partition level 3. In TABLE III, we embed the secret n-bit (n=1 or 2) message m in each pixel. At the same block size and partition level, secret 2-bit has more embedding capacity than secret 1-bit. Unfortunately, PSNR of secret 2-bit will be reduced due to increasing amount of capacity. Therefore, PSNR and capacity are usually in conflict. If the embedding capacity is improved, the PSNR will drop and vice versa. Thus, a tradeoff between the data embedding capacity and PSNR of the marked image is an important issue for a target application. According to experiments in TABLE I, TABLE II, and TABLE III, we can adjust the block size, partition level, and n-bits in secret message to meet the requirements of PSNR and capacity for specific applications. From Figure 11(a), secret 2-bit message m in each pixel has better quality than secret 1-bit because PSNR-Capacity curve of secret 2-bit is smooth. When the amount of capacity is 100,858 in secret 2-bit, which is almost two times compared with 1-bit, PSNR value is still acceptable in 69.65. Apparently, the more capacity, the less PSNR. At the block size 5, the amounts of capacity of secret 2-bit will be increased dramatically than those of secret 1-bit as shown in Figure 11(b). In general, the smaller block size, the higher amount of capacity. As the same block size, secret 2-bit obtains lower values of PSNR than those of secret 1-bit as shown in Figure 11(c). In Figure 11(d) the

higher block size, the lower optimal threshold k. The following (TABLE IV) are some test examples. We applied the data embedding to 32 slices from the National Cancer Imaging Archive with sign 16-bit depth image. All PSNR are above 61 dB. On the sing 16-bit depth, the optimal block size is 2×2 because the capacity is the largest and also have higher PSNR shown in TABLE IV. On the unsign 16-bit depth, the optimal block size is 2×2 for the values of PSNR are acceptable about 74.

Considering underflow/overflow problem, we test on sign 16-bit-depth (TABLE I~TABLE IV) and unsign 16-bit depth medical images (TABLE V~TABLE VI). Because of high bit-depth, small range of intensity, and small value of underflow/overflow, the utilization rate is very low. Therefore, there is no underflow/overflow problem in sign 16-bit depth (TABLE I~TABLE IV) medical images. For unsign 16-bit depth, underflow problem will be processed shown in TABLE V and TABLE VI. In the block size 2×2, the maximum of underflow is -11 shown in TABLE V. After shifting image histogram to rightward for underflow process, the PSNR will be above 74. In order to preserve smooth surface structure in volume of medical images, we use the Inter-Slice PSNR to measure the neighbor pixels of difference intensity between two slices shown in TABLE VI. In general, the best quality of smooth surface will have higher Inter-Slice PSNR.

5. Conclusions and Discussion

We have proposed a novel reversible image data hiding scheme by applying difference bit-embedding strategies in high bit-depth of volume structure on medical images. Until now, most of reversible data hiding schemes are still designed to apply on a single medical image. However, many of medical images have volume structures produced by medical scanners. In this paper, we propose six criteria for reversible data hiding scheme in medical images. Singn and unsign 16-bit depth high quality medical images with dicom format are tested on our algorithm. Because adopting block based with shift histogram, our embedding method can distribute secret bits to whole images with copy

attack avoidance. Thus, our method is well-suited for high quality medical images and without salt-and-pepper. We apply the utilization rate and histogram shift to solve underflow/overflow problem. Our scheme satisfies the criterion of free location map because shift distance is the only parameter to be recorded. Our algorithm is applied in volume structure medical images. For preserving smooth surface of anatomical structure to reassemble image slices as a volume of 3D medical images, we define the Inter-Slice PSNR to measure the distance between neighbor pixels and adjust block size, threshold k , and number of embedding bits to improve smooth surface quality. Because pixels of a block are highly correlated and exhibit strong spatial redundancy, our scheme applied blocks of difference pair pattern to create a free space for embedding secret bits. Thus, our scheme performs on sparse histogram of intensity very well.

We compare several other histogram shifting based methods with our method in TABLE VII described as follows. Our algorithm has satisfied all criteria in TABLE VII. Ni et al. [24] scheme applied difference pair patterns to hide data. Because embed bit is “0” or “1” by shifting the same histogram in

TABLE VII. The comaprison of data hiding schemes

Criteria	Our scheme (1)	Ni et al. scheme [24] (2)	Luo et al. scheme [19] (3)	Chang et al. scheme [4] (4)	Vleeschouwer et al. scheme [31] (5)
1. Well-suited for high quality medical images	Yes	Yes	Yes	No	Yes
2. Without salt-and-pepper	Yes	Yes	Yes	Yes	No
3. Applicable to medical image with smooth surface	Yes	No	No	No	No
4. Well-suited for sparse histogram of intensity levels	Yes	Yes	Yes	No	Yes
5. Free location map	Yes	Yes	No	Yes	Yes
6.Ability of adjusting data embedding capacity, PSNR, Inter-Slice PSNR	Yes	No	No	No	No
7. Without error correction	Yes	No	Yes	Yes	Yes

bit-embedding process, some mistakes have to be corrected by error correction coding such as BCH(63,7,15) at extraction stage. Adopting difference pairs pattern with partition level, our scheme has no errors because embed bits “0” or “1” are shifted to different histogram bins. In the reversible data hiding aspect, our scheme is the first paper to propose smooth surface preserving on volumes of medical images for 3D model reconstruction. The others of schemes only test on single image. Luo et al. has location map to record the underflow/overflow position. Chang et al. utilize the continuous duplicate values to embed secrets. Therefore, this scheme does not match the criteria 1, 3, 4, 6. Applying the modulo-256 addition method to process underflow/overflow problem, Vleeschouwer‘s scheme will produce salt-and-pepper.

Acknowledgements

We would like to thank National Cancer Institute for pro-viding the CT image data used in this study. Thanks also go to the National Science Council of ROC for supporting this work in part under Contract NSC 98-2221-E-126-014-MY3.

References

[1] A. M. Alattar, “Reversible watermark using the difference expansion of a generalized integer transform,” IEEE Trans. Image Process., vol. 13, pp. 1147-1156, 2004.

[2] Doug M. Boyer, Yaron Lipman, Elizabeth St. Clair, Jesus Puente, Biren A. Patel, Thomas Funkhouser, Jukka Jernvall, and Ingrid Daubechies, “Algorithms to automatically qantify the geometric similarity of anatomical surfaces,” Proc. of the National Acasemy of Sciences of the United States of America, vol. 108, no. 45, pp. 18221-18226.

[3] Shu-Fen Chiou, I-En Liao, and Min-Shiang Hwang, “A capacity-enhanced reversible data hiding scheme based on SMVQ”, The Imaging Science Journal, vol. 59, no. 1, pp. 17-24, 2011.

[4] Zhiguo Chang and Jian Xu, “Reversible run length data embedding for medical images,” Communication Software and Networks (ICCSN), IEEE 3rd International Conference, pp. 260-263, 2011.

[5] Jen-Bang Feng, Iuon-Chang Lin, Chwei-Shyong Tsai, and Yen-Ping Chu, "Reversible watermarking: current status and key issues," International Journal of Network Security, vol. 12, no. 3, pp. 161-171, 2006.

[6] M. Fallahpour, D. Megias, and M. Ghanbari, "Reversible and high-capacity data hiding in medical images," IET Image Process, vol. 5, Iss. 2, pp. 190-197, 2011.

[7] Masaaki Fujiyoshi, Shuji Sato, Hong Lin Jin, and Hitoshi Kiya, "A location-map free reversible data hiding method using block-based single parameter," IEEE International Conference on Image Processing, vol. 3, pp. III-257-III-260, 2007.

[8] Masaaki Fujiyoshi, Takahiro Tsuneyoshi, and Hitoshi Kiya, "A reversible data hiding method free from loaction map and parameter memorization," International Symposium on Communications and Information Technologies, pp. 767-772, 2010.

[9] Miroslav Goljan, Jessica J. Fridrich, and Rui Du, "Distortion-free data embedding for images," Proc. 4th Information Hiding Workshop, Pittsburgh, PA, pp. 27-41, 2001.

[10] B. K. Gunturk, Y. Altunbasak, and R. Mersereau, "Gray-scale resolution enhancement," IEEE Forth Workshop on Multimedia Signal Processing, pp. 155-160, 2001.

[11] Rafael C. Gonzalez and Richard E. Woods, "Digital image processing," Second Edition, 2002.

[12] Hsiang-Cheh Huang and Wai-Chi Fang, "Integrity preservation and privacy protection for medical images with histogram-based reversible data hiding", Life Science System and Applications Workshop, pp. 108-111, 2011.

[13] Yongjian Hu, Heung-Kyu Lee, and Jianwei Li, "DE-based reversible data hiding with improved overflow location map," IEEE Trans. on Circuits Systems for Video Technology, vol. 19, no. 2, pp. 250-260, 2009.

[14] Seungwu Han, Masaaki Fujiyoshi, and Hitoshi Kiya, "A reversible image authentication method without memorization of hiding parameters," IEICE Transactions, vol. E92-A, Iss. 10, pp. 2572-2579, 2009.

[15] Li-Chin Huang, Lin-Yu Tseng, and Min-Shiang Hwang, "The study of data hiding in medical image," International Journal of Network Security, vol. 14, no. 5, pp. 243-252, 2012.

[16] Behrang Mehrbany, Xin Cindy Guo, and Dimitrios Hatzinakos, "A high capacity reversible multiple watermarking scheme for medical images," IEEE Digital Signal Processing , pp.1-6, 2011.

[17] Hyoung Joong Kim, V. Sachnev, Yun Qing Shi, Jeho Nam, and Hyon-Gon Choo, "A novel difference expansion transform for reversible data embedding," IEEE Trans. Information Forensics and Security, vol. 3, no. 3, pp. 456-465, Sep. 2008.

[18] Ching-Chiuan Lin, Shun-Ping Yang, and Nien-Lin Hsueh, "Lossless data hiding based on difference expansion without a location map," in 2008 Congress on Image and Signal Processing, p p. 8-12, 2008.

[19] Hao Luo, Fa-Xin Yu, Hua Chen, Zheng-Liang Huang, Hu Li, Ping-Hui Wang, "Reversible data hiding based on block median preservation," Information Sciences, vol. 181, pp. 308-328, 2011.

[20] Der-Chyuan Lou, Ming-Chiang Hu, Jiang-Lung Liu, "Multiple layer data hiding scheme for medical images," Computer Standard and Interfaces, vol. 31, Iss. 2, pp. 329-335, 2009.

[21] Hui-Chieh Lu, Yen-Ping Chu, Min-Shiang Hwang, "A new Steganographic method of the pixel-value differencing," The Journal of Imaging Science and Technology, vol. 50, no. 5, pp. 424-426, 2006.

[22] Tim Mclnerney and Demetri Terzopoulos, "Topology adaptive deformable surfaces for medical image volume segmentation," IEEE Trans. on Medical Imaging, vol. 18, no. 10, pp. 840-850, 1999.

[23] Zhicheng Ni, Yun-Qing Shi, Nirwan Ansari, and Wei Su, "Reversible data hiding," IEEE Trans. on Circuits Systems for Video Technology, vol. 16, pp. 354-362, 2006.

[24] Zhichen Ni, Yun Q. Shi, Nirwan Ansari, Wei Su, Qibin Sun and Xiao Lin, "Robust lossless image data hiding designed for seim-fragile image authentication," IEEE Trans. on Circuits Systems for Video Technology, vol. 18, pp.497-509, 2008.

[25] National Cancer Imaging Archive. Available at https://imaging.nci.nih.gov/.

[26] Joan Bartrina-Rapesta, Joan Serra-Sagrista, Francesc Auli-Llinas, and Juan Munoz Gomez, "JPEG2000 ROI coding method with perfect fine-grain accuracy and lossless recovery," Conference Record of the Forty-Third Asilomar Conference on Signals, Systems and Computers, pp. 558-562, 2009.

[27] Roman Starosolski, "Compressing high bit depth images of sparse histograms," International Electronic conference on Computer Science, pp. 269-272, 2007.

[28] Roman Starosolski, "Compressing images of sparse histograms," Proc. SPIE, Medical Imaging, vol. 5959, pp.209-217, 2005.

[29] Roman Starosolski, "Performance evaluation of lossless medical and natural continuous tone image compression algorithms," Proc. SPIE, Medical Imaging, vol. 5959, pp. 116-127, 2005.

[30] J. Tian, "Reversible data embedding using a difference expansion," IEEE Trans. Circuits and Systems for Video Technology, vol. 13, no 8, pp. 890-896, 2003.

[31] Piyu Tsai, Yu-Chen Hu, and Hsiu-Lien Yeh, "Reversible image hiding scheme using predictive coding and histogram shifting," Signal Processing, vol. 89, pp. 1129-1143, 2009.

[32] Christophe De Vleeschouwer, Jean-Francois Deloaigle, and Benoit Macq, "Circular interpretation of bijective transformation in lossless watermarking for media asset management," IEEE Trans. on Multimedia, vol. 5, pp. 97-104, 2003.

[33] Chia-Chun Wu, Shang-Juh Kao, and Min-Shiang Hwang, "A high quality image sharing with steganography and adaptive authentication scheme," The Journal of Systems and Software, vol. 84, pp. 2196-2207, 2011.

[34] Zhiqiong Wang, Xianfeng Meng, Yue Zhao, Hongehi Xue, Qianxi Li, Jinag Li, Tianjing Zhang, and Yuhua Chen, "Lung lobe segmentation based on HRCT data," International Conference on Biomedical Engineering and Computer Science, pp. 1-4, 2010.

[35] Chung-Ming Wang, Nan-I Wu, Chwei-Shyong Tsai and Min-Shiang Hwang, "A high quality steganographic method with pixel-value differencing and modulus function," The Journal of Systems and Software, vol. 81, Iss. 1, pp. 150-158, 2008.

[36] Q. Wei, Y. Hu, H. MacGregor, and G. Gelfand, "Identification of Lobar Fissures in pathological lungs," 32nd Annual International Conference of the IEEE EMBS, pp. 5347-5350, 2010.

[37] Terry S. Yoo, Bryan Morse, K. R. Subramanian, Penny Rheingans, Michael J. Ackerman, "Anatomic modeling from unstructured samples using variational implicit surfaces," Proc. ACM SIGGRAPH Courses Article no. 245, 2005.

[38] Li Zhang, Eric A. Hoffman, and Joseph M. Reihardt, "Atlas-driven lung lobe segmentation in volumetric X-ray CT images," IEEE Trans. on Medical Imaging, vol. 25, no. 1, pp. 1-16, 2006.